Hair Follicle Epithelial Stem Cells Contribute to Interfollicular Epidermis during Homeostasis

Elnaz Ghotbi[1,#], Edem Tchegnon[1,#], Ze Yu[2], Tracey Shipman[1], Zhiguo Chen[3], Yumeng Zhang[3], Renee M. McKay[3], Chao Xing[2,4,5], Chung-Ping Liao[1,6], and Lu Q. Le[1,3,*]

[1]Department of Dermatology, University of Texas Southwestern Medical Center, Dallas, TX 75390, USA
[2]McDermott Center for Human Growth and Development, University of Texas Southwestern Medical Center, Dallas, TX 75390, USA
[3]Department of Dermatology, University of Virginia, Charlottesville, VA, 22903
[4]Department of Bioinformatics, University of Texas Southwestern Medical Center, Dallas, TX 75390, USA
[5]O'Donnell School of Public Health, University of Texas Southwestern Medical Center, Dallas, TX 75390, USA
[6]Graduate Institute of Medical Sciences, College of Medicine, Taipei Medical University, Taipei, Taiwan

# These authors contributed equally

*Author for Correspondence:
Lu Q. Le, MD, PhD
Professor and Chair
Department of Dermatology
University of Virginia School of Medicine
Charlottesville, VA, USA
Email: bkn6qd@uvahealth.org

Running title: Epithelial Stem Cell Population for Interfollicular Epidermis

Keywords: Stem Cell Niche, Interfollicular Epidermis Stem Cell, IFE, Epidermal Stem Cell, Skin Stem Cell, *Krox20*, *EGR2*.

Declaration of Interests

The authors declare no competing interests.

Summary

Mammalian skin is a vital barrier with the epidermis serving as its protective outer layer, continually undergoing renewal. Given that loss of the epidermis or its barrier function is lethal for mammals, multiple stem cell populations likely exist for the interfollicular epidermis (IFE), enhancing evolutionary survival. Here, we demonstrate that transcription factor KROX20 marks a heterogeneous stem cell population in the upper and middle mouse hair follicle (HF), partially overlapping with known HF stem cell markers in those regions. Lineage tracing in mice using different reporter lines shows that *Krox20*-lineage cells migrate from the HF to the IFE, contributing to both basal and suprabasal layers during adulthood. Spatial transcriptomics data corroborate our findings. Depletion of epithelial *Krox20*-expressing cells leads to epidermal hyperplasia and a disruption of stratification during morphogenesis and homeostasis. Our study highlights the contribution of hair follicle *Krox20*-lineage cells to the IFE and the regulation of epidermal homeostasis.

Introduction

The mammalian skin functions as a crucial mechanical and biological safeguard. The skin's epidermis comprises a basal layer with actively dividing cells and several suprabasal layers that undergo differentiation and enucleation as they migrate upward, ultimately leading to the formation of a cornified layer that is eventually shed from the skin surface (1). In maintaining homeostasis, the loss of epidermal cells during terminal differentiation must be precisely compensated for by the generation of new cells in the basal layer. One study suggests that the epidermis is sustained by a single proliferating committed progenitor cell population, where the balance between proliferation and differentiation results from random cell division fates (2). Conversely, another study indicates the presence of two distinct populations of epidermal progenitors in the basal layer of the interfollicular epidermis (IFE): a stem cell population and a progenitor cell population, each contributing differentially to the homeostasis of the epidermis (3). Prior research demonstrates that the epidermis and hair follicles (HFs) are maintained by local stem and progenitor cells in a compartmentalized manner during homeostasis (4). Stem cells within the epidermis are primarily located in the basal layer of the epithelium, identifiable by the basal keratins K5 and K14 (5). However, considering that the loss of the epidermis or its barrier function is incompatible with mammalian life (6), the existence of multiple stem cell populations for the IFE is likely, as this would enhance evolutionary survival. We previously reported *Krox20* (*Egr2*) as a marker for a population of epithelial cells in the HF that contribute to the formation of bulge (7) and hair shaft (8). Here, we demonstrate that *Krox20*-lineage cells also contribute to the IFE during homeostasis, introducing *Krox20*-positive stem cells as a population contributing to both HF and IFE.

Results

Krox20-expressing cells are a heterogeneous population of epithelial stem cells in the upper hair follicle

KROX20 is a zinc finger transcription factor critical for the development and homeostasis of multiple tissues. Previous studies have documented the presence of *Krox20* in HFs during embryogenesis and early development, initiating at E14.5 (8, 9). Employing *Krox20-GFP* mice (which recapitulate endogenous *Krox20* expression (10)) to visualize the expression of GFP, and using a KROX20 antibody in immunofluorescence assays, we demonstrated that *Krox20* is expressed predominantly in the HF infundibulum and spans from the upper to middle regions of the telogen and anagen HFs and extends to the sebaceous glands (7) (Supplemental Figures 1A and 1B). This expression pattern within the HFs, coupled with its spatial co-localization with established stem cell markers such as *Lrig1* and *Lgr6* (4, 7), implies a substantial level of heterogeneity within this stem cell pool.

To investigate this further, we conducted single-cell RNA sequencing (scRNA-seq) on *Krox20*-positive cells from epidermal cells of the skin of P5 *Krox20-GFP* mice. The analysis revealed 10 distinct clusters with differentially expressed genes, confirming the heterogeneity of *Krox20*-positive cells (Figure 1A). Cell type annotations based on known gene markers identified basal and differentiating keratinocytes, upper hair follicle, and sebaceous glands (Figure 1B). This distribution corresponded to the expression domain in the upper HF and sebaceous gland as shown in our immunofluorescence assays (Supplemental Figures 1A and 1B) (7). As expected, *Krox20* expression overlapped with known upper and middle HF stem cell markers, particularly with *Lrig1*, *Lgr6*, *GATA6*, *Krt79* and to a lesser extent, *Sca1* (Figures 1C and 1D). Additionally, *Nestin* expression was largely absent from these *Krox20*-positive populations, with only a very small

fraction of cells showing co-expression. Given that *Nestin* expression has been reported in the bulge region (11, 12), this minimal overlap confirms that *Krox20* is not expressed in the bulge (Figures 1C and 1D).

***Krox20*-lineage cells contribute to IFE during homeostasis**

To trace the lineage fate of *Krox20*-positive cells, we generated an inducible *Krox20-CreERT* knock-in mouse line as previously described (7). We used CRISPR/Cas9 to insert *CreERT* after exon 2 of *Krox20* following a P2A linker, thus keeping *Krox20* expression/ function intact. We then bred *Krox20-CreERT* mice with *R26-tdTomato* reporter mice to generate *Krox20-CreERT; R26-tdTomato* mice. We excluded the potential for leakiness in this mouse line, as no *tdTomato* signal was observed in the absence of tamoxifen treatment (7) (Supplemental Figure 1C). However, one challenge in lineage tracing a heterogeneous population of cells is that performing the tracing at the clonal level, such as labeling a single cell and tracing its progeny, may not accurately represent the true capabilities or characteristics of the broader population of cells, even with multiple replicates.

In our lineage tracing analysis with *Krox20-CreERT; R26-tdTomato* mice, we induced labeling to the extent that we observed most *Krox20*-expressing cells labeled at the onset of our lineage tracing analysis (Figures 2A and 2B). This approach ensures that the full range of behaviors/ fates that are possible in the entire population of *Krox20*-expressing cells will be captured. Therefore, mice were induced with 40 µg 4-hydroxytamoxifen at P1, and their skin was subsequently examined at different time points, spanning from three to 119 days post-induction (Figure 2A). At P4, three days post-induction, *Krox20*-lineage cells were confined to the expression domain of *Krox20* in the upper and middle regions of the anagen HF. However,

Krox20-lineage cells were detected in the bulge and IFE by P30, and the contribution of lineage-traced cells to these regions increased in subsequent hair cycles (Figure 2A).

When tamoxifen induction was initiated later in development at 8 weeks of age, which corresponds to the second long and synchronous telogen phase of the hair cycle (P55–P56), and HFs were examined 3 days later, the *tdTomato*-expressing cells remained confined to the upper and middle telogen HFs (Figure 2B, P58), closely resembling the "live" expression pattern observed with *Krox20*-GFP (Supplemental Figure 1A). The lineage cells were detectable in the IFE by 30 days (Figure 2B, P85) and were expanding by 59 days post-gavage (Figure 2B, P114). By 18 weeks post-induction, the lineage cells were detected in both the bulge and IFE (Figure 2B, P175). When tamoxifen induction was performed following multiple hair cycles at P98-P101, the *tdTomato*-expressing cells remained confined to the upper and middle telogen HFs when examined two days after induction (Figure 2C, P100). Subsequently, these cells extended down the HF, partially reaching the bulge region by 11 weeks (Figure 2C, P175). By 16 weeks post-induction, the lineage cells expanded their occupancy of the bulge while also contributing to the IFE (Figure 2C, P210). These findings provide conclusive evidence that *Krox20*-lineage cells continue to populate the postnatal IFE perinatally and throughout adulthood. The quantification of *Krox20*-lineage cells labeled by *tdTomato* in the IFE in *Krox20-CreERT; R26-tdTomato* mice induced at P1, P55, and P98 is shown in Supplemental Figure 2A, B, and C, respectively.

Immunostaining of *tdTomato* together with IFE markers, including K14 for the basal layer and Loricrin (Lor) for the suprabasal layers of IFE, revealed the co-localization of *Krox20*-lineage cells with both basal and suprabasal layers of IFE (Figures 3A and B). This suggests the migration of *Krox20*-lineage cells from the HF to the basal layer of IFE, where they subsequently undergo differentiation, migrate to the suprabasal granular layer, and express Lor. Furthermore, *Krox20*-

lineage cells co-localize with the Ki67 proliferation marker in the basal keratinocytes of IFE and hair follicles, indicating that *Krox20*-lineage cells contain actively cycling cells (Figure 3C). Lineage tracing using *Krox20-Cre; R26-tdTomato* mice yielded similar findings, with *tdTomato* labeling the upper part of the HFs during the perinatal period (late gestation E18.5 and early postnatal P5), before migrating to the IFE by P30 (Supplemental Figure 3A and 3B). Our lineage tracing findings provide strong evidence that *Krox20*-lineage cells in the IFE originate from the HF. Given that epithelial *Krox20*-positive cells represent a subgroup of embryonic *K14*-positive cells(8), this finding suggests that *Krox20*-lineage cells may reactivate *K14* expression once they migrate to the basal layer of the IFE to contribute to skin homeostasis.

Comprehensive validation of lineage tracing interpretation through multiple alternative approaches

Our lineage tracing studies revealed that *Krox20*-expressing cells within the HF contribute to the IFE. However, interpreting such data requires caution, as previous studies have shown discrepancies in marker and/or reporter expression. For instance, *Lgr6*-positive cells, initially believed to be a stem cell marker of the HF isthmus, were reported to contribute to the formation of the HF, sebaceous gland, and IFE (13). However, later studies reported the expression of *Lgr6* in IFE and sebaceous glands, questioning the validity of the lineage tracing results in the initial study (4, 14). Additionally, another study demonstrated the detection of YFP in the basal layer of the IFE one week after induction using *Involucrin-CreER; R26-YFP* mice, despite the absence of involucrin protein expression in the immunostaining assay (3). Therefore, there remains the possibility that very low levels of *Krox20*, and consequently *CreERT*, are expressed in the IFE but

fall below the detection capability of our current methods, leading to the detection of *tdTomato* in the IFE rather than the migration of *Krox20*-lineage cells.

To address this concern and confirm the interpretation of our lineage tracing data, we took a multipronged approach to rule out this possibility. Utilizing the tamoxifen-inducible *Krox20-CreERT* line for lineage tracing adds a layer of confidence that the labeling of the IFE, which begins long after tamoxifen administration (a month after the tamoxifen induction at P1 and 112 days after the induction at P98), represents the migration of *Krox20*-lineage cells and is not due to the expression of *CreERT* in these regions.

However, even with inducible *CreERT* lines, a low level of leakiness/ background activity of basal *CreERT* is possible, which could result in reporter activation occurring independently of tamoxifen induction (15). In this regard, reporter lines such as *mTmG* and *R26-YFP* were shown to be more faithful reporters, exhibiting a higher recombination threshold for basal *CreERT* leakage compared to *R26-tdTomato* (15). While the possibility of background activity of *CreERT* in our *Krox20-CreERT; R26-tdTomato* was already excluded (7) (Supplemental Figure 1C and 1D), to confirm the interpretation of our lineage tracing findings obtained using the *R26-tdTomato* reporter line, we repeated these experiments using *R26-YFP* reporter mice. These mice were administered a single dose of 4-hydroxytamoxifen (at P3) and subsequently underwent skin analysis at two different time points: 14 days and 43 days post-induction. At two weeks after tamoxifen treatment, the *Krox20*-lineage cells in the *Krox20-CreERT; R26-YFP* mice were predominantly localized to the upper HF (Supplemental Figure 4A). However, by P43, the *Krox20*-lineage cells were detected at the bulge and IFE regions (Supplemental Figure 4B). These findings confirm the results obtained from the lineage tracing experiment conducted with *Krox20-CreERT; R26-tdTomato* mice. Of note, all lineage tracings conducted with *Krox20-CreERT* and the two

different reporter lines (*R26-YFP* and *R26-tdTomato*) consistently demonstrated that the labeling of the IFE initiates/ extends from the HF "mouth". From this point, the labeling extended contiguously, marking the IFE. This labeling pattern is consistent and reproducibly observed, providing a robust basis for our observation regarding the HF origin of a specific subset of stem cells within the IFE.

We further evaluated the contribution of *Krox20*-lineage cells to IFE when lineage tracing is initiated at various, yet overlapping ages, using the inducible *Krox20-CreERT; R26-tdTomato*. When tamoxifen induction was performed perinatally (at P1), *Krox20*-lineage cells were observed in the IFE by P30 (Figure 2A). However, the contribution of these lineage-traced cells to these regions increased in subsequent hair cycles (Figure 2A). When tamoxifen induction was performed between P98-101, *Krox20*-lineage cells were primarily detected in the upper HF at 2-days post-induction, with virtually no presence in the bulge and IFE (Figure 2C). Conversely, in mice at a similar age (P100), but induced at P1, *Krox20*-lineage cells were already detected at bulge and IFE regions (Figure 2A). The difference between these results demonstrates that the *tdTomato* signal detected in the bulge and IFE reflects the progeny of *Krox20*-positive cells, rather than representing live *Krox20* expression in these regions. Conducting the lineage tracing in $n \geq 4$ replicates and consistently detecting *tdTomato* signal within the IFE at approximately the same time points among the replicates strengthens our claim that *Krox20*-lineage cells in the IFE migrated upward from the HF.

Previous research has revealed fate plasticity for various epidermal stem cells in response to injury or during wound healing (16, 17). To exclude the possibility of micro-wounds or small abrasions from mice scratch, influencing the migration of *Krox20*-lineage cells to IFE, female and

male mice, housed separately in cages without cohabitation, were utilized for a number of replicates for lineage tracing assays in this study.

To further ensure the accuracy of our lineage tracing results and to avoid potential over-interpretation due to *CreERT* expression in the IFE, we employed spatial transcriptomics to analyze the precise expression pattern of *Krox20* and *CreERT*. Dorsal skin samples were collected from *Krox20-CreERT; R26-tdTomato* mice at P38 (n=3), induced at P2, with each mouse corresponding to one skin section per slice (Figure 4A). This approach identified 12 clusters of cells with differentially expressed genes (Figure 4B). Cluster 2 was identified as the IFE (Figure 4B); however, due to the resolution limitations of the technique, we were unable to distinguish between basal and suprabasal layers within the IFE as well as the bulge area from the nearby middle HF regions. The spatial feature plot of *CreERT* expression in different regions of HF and skin is shown in Figure 4C. Dot plots in Figure 4D illustrate the expression of *CreERT* and *Krox20*, along with other IFE markers (*K14*, *K15*, *K1*, *Sca1/Ly6a*, *Thy1*, and *loricrin*), *Lrig1* (a marker of the upper HF) and *Nestin*, (11, 12) in different clusters. Our analysis of *Krox20* expression in the IFE revealed that approximately 35% of cells in cluster 2 exhibited *Krox20* expression (scaled average expression of 0.43) (Figure 4D). The dot plots demonstrated a correlation between *Krox20* and *CreERT* expression across various clusters, with *CreERT* expression levels being lower than those of *Krox20* (Figure 4D). This aligns with the immunostainings performed with CRE antibody on the skin sections from *Krox20-CreERT; R26-tdTomato* mice induced at P1 and analyzed at P22 (Supplemental Figure 5A), and P37 (Supplemental Figure 5B), which showed low intensity of CRE signals. Notably, no CRE staining was detected in the IFE at P37, the time point when the IFE was labeled by *tdTomato* (Supplemental Figure 5B).

Importantly, *Nestin* expression was detected in clusters corresponding to lower and mid-HF regions. While *Krox20* and *Nestin* showed limited co-expression, their spatial expression patterns were largely distinct (Figure 4D), suggesting that they mark separate cell populations within the follicle consistent with our single-cell RNA-seq data in Figures 1C and 1D.

Previous studies have suggested decreased protein expression at the position downstream of P2A in bicistronic constructs (18). Therefore, the lower expression level of *CreERT* compared to *Krox20* is likely attributed to the design of the *Krox20-CreERT* line, which contains *CreERT* downstream of a P2A linker (7). While *tdTomato* labeling was observed extending from the HF mouth in the IFE at this age (P38, Figure 4E), the dot plot analysis indicated that *CreERT* expression was restricted to the main expression domain of *Krox20*, which is in the upper HF, and was absent from other regions of the epidermis, including the IFE (scaled average expression of 0.28) (Figure 4D). This observation rules out the possibility of unintended activation of *tdTomato* due to the background activity of *CreERT* and provides strong evidence that, while *Krox20* is expressed at low levels and in a subset of cells in the IFE, *tdTomato* labeling of the IFE represents *Krox20*-lineage cells that have migrated from the HF upward to contribute to the IFE.

The conclusion from our lineage tracing studies is directly supported by a recent study demonstrating that cells from the upper HF progressively integrate into the IFE and modulate skin barrier function (19). This independent validation strengthens our findings and confirms the HF as a cellular reservoir for the IFE, reinforcing the validity of our observations.

***Krox20*-lineage cells do not contribute to volar skin**

In both human and mouse, the majority of skin surfaces are associated with HFs, with major exceptions being the hairless and thickened skin of the palm and sole (volar skin). Since *Krox20*-

positive cells mark a population of epidermal stem cells within the HF, we performed lineage tracing in volar skin of *Krox20-CreERT; R26-tdTomato* mice, inducing at P1 and analyzed at 11M (Figure 5A), and inducing at P55 and analyzing at P158 to determine whether *Krox20*-lineage cells are detected in volar epidermis. We observed a distinct discontinuation of *Krox20*-lineage cells at the junction of hairy and hairless IFE (Figure 5A and 5B), suggesting that the *tdTomato* labeling of the IFE has a HF origin. These findings show that *Krox20*-positive cells exclusively serve as the stem cells for hairy epidermis and suggest the existence of other stem cell populations within the IFE that are responsible for maintaining the homeostasis of volar epithelia.

Krox20-positive cells are indispensable for skin homeostasis

To determine the effect of ablating *Krox20*-positive cells on the skin during homeostasis, we eliminated *Krox20*-expressing cells in the skin by breeding mice with the *Krox20-lox-Stop-lox-DTA* (*Krox20-DTA*) knock-in allele (10) with a *K14-CreERT* line (20), generating *Krox20-DTA; K14-CreERT* mice. In this model, *Krox20*-expressing cells of the *K14* lineage express diphtheria toxin A (DTA) and are ablated upon gavage with tamoxifen. Using this model, we ablated epithelial *Krox20*-expressing cells in the skin of mice at P32, which approximately corresponds to the time point when *Krox20*-lineage cells begin migrating to the IFE (Figures 6A and 6B). The analysis of the skin 9 days after the ablation at P32 (P41), showed that depletion of *Krox20*-expressing cells resulted in hyperplasia of the epidermis (Figures 6A and 6B). To determine the cause of epidermal hyperplasia in these mice, we first analyzed the basal cell marker K14. Strikingly, K14 was expressed in the entire epidermis of mutant mice, and the K14-positive layer was markedly thicker. We then explored the effect of *Krox20*-positive cell deletion on the bulge, as well as the basal and suprabasal layers of IFE by immunostaining for K15, a marker for both

the bulge and basal layer of stratified epithelium (21, 22) and loricrin (LOR), a marker of suprabasal granular cells. Notably, the elimination of epithelial *Krox20*-positive cells led to the loss of *K15*-positive epidermal stem cells in IFE (Figure 6A). In control epidermis, the loricrin layer exists as a discrete layer superficial to the K14-positive basal layer (Figure 6B). However, in the absence of *Krox20*-positive cells, the loricrin layer overlapped with the K14 layer within the suprabasal layer (Figure 6B). These findings demonstrate that the loss of *Krox20*-positive cells disrupts normal epidermal stratification and suggest an essential role for *Krox20*-expressing cells in maintaining skin homeostasis in adulthood.

A potential contributing factor to the epidermal hyperplasia observed in our model may be an inflammatory response triggered by hair follicle degeneration. To explore this possibility, we conducted immunofluorescence analyses targeting specific immune cell markers, CD3 for T cells, CD4 for helper T cells, CD8 for cytotoxic T cells, and IBA1 for macrophages (Supplemental Figure 6A–D). Among these, only IBA1 staining showed a notable increase, indicating enhanced macrophage presence in the dermis of *Krox20-DTA; K14-CreERT* mice. In contrast, we found no substantial evidence of infiltration by other immune cell types. These results point toward a localized macrophage response rather than a broad immune cell recruitment. Whether this macrophage accumulation is a driving factor in the development of hyperplasia or a downstream effect of tissue disruption remains an open question that warrants further investigation.

KROX20 expression regulates cell fate determination by preventing epithelial differentiation

Given the epidermal hyperplasia phenotype observed as the result of ablating *Krox20*-positive cells in *K14*-expressing cells, we investigated the functional role of KROX20 in epithelial cells by overexpressing *Krox20* in vitro. The pLVX lentiviral vector containing mouse *Krox20* cDNA and

IRES-ZsGreen1 and its corresponding control vector which expresses only ZsGreen were used for transfection to overexpress *Krox20* in HEK293T and HHFK cells, human embryonic kidney and human hair follicular keratinocyte cells, respectively.

In HEK293T cells, overexpression of *Krox20* caused morphological changes by 5 days post-transfection, resulting in a more rounded morphology (Figure 7A). However, by 23 days post-transfection, the overexpressing cells regained a normal morphology identical to that of the control cells (Figure 7A). However, due to the lack of proliferation in *Krox20*-overexpressing HHFKs, analysis of HHFK cells beyond 4 days post-transfection was not possible (Figure 7B).

We hypothesized that the observed morphological change in HEK293T cells could indicate that the cells were undergoing either apoptosis or a change in cell identity. To assess apoptosis, we evaluated the levels of apoptotic markers BIM and Cleaved Caspase-3. Western blot analysis demonstrated a lower level of these apoptotic markers in *Krox20*-overexpressing HEK293T cells compared to their control counterparts (Figure 7C). Interestingly, *Krox20*-overexpressing HHFKs also caused downregulation of the apoptotic markers within 4 days post-transfection (Figure 7C). To investigate if the cells were undergoing an identity change, we evaluated the expression level of various epithelial versus mesenchymal markers using RT-qPCR (Figure 7D). The *Krox20*-overexpressing HHFKs cells showed varying expression levels of these genes, including a significant upregulation of *Snail1*, *Twist1*, *β-catenin*, and *Notch1*, regulators of epithelial-mesenchymal transition (EMT) (23-26), and a downregulation of *E-Cadherin*, a marker of epithelial cells (27, 28) (Figure 7D). While these results do not establish a direct role for endogenous KROX20, they raise the possibility that *Krox20* overexpression may influence pathways involved in epithelial differentiation and survival, warranting further investigation in more physiologically relevant systems.

Discussion

In this study, we showed that transcription factor KROX20 marks a population of stem cells expressed in the upper and middle HF that contribute to IFE. Interestingly, our research indicated that depletion of *Krox20*-positive cells of the *K14* lineage leads to hyperplasia, marked by a clear expansion of *K14*-positive cells, and aberrant differentiation/stratification of the IFE in adult mice (Figure 6). This suggests that *Krox20*-lineage cells play an important role in maintaining proper epidermal homeostasis. One potential explanation for the observed epidermal hyperplasia is the presence of other resident stem cell populations in the IFE that either counteract or overcompensate for the loss of *Krox20*-lineage cells.

Previous studies have demonstrated that HF stem cell populations can contribute to IFE regeneration, but this has mostly been observed under non-homeostatic conditions (29-32). The most compelling evidence for the absence of HF lineage cells in the IFE comes from *Shh*- and *Sox9*-lineage tracing analyses (33, 34). In these studies, the majority of the HF is labeled, indicating the presence of lineage cells, while the IFE remains unlabeled. These findings, however, can be reconciled with our results. In the case of *Shh*-lineage analysis, a notable observation is the absence of these cells in the majority of the infundibulum (34), the dominant region of *Krox20* expression in the HF. This suggests that the unlabeled cells may actually represent *Krox20*-positive cells with the capacity to regenerate the IFE. On the other hand, starting at ~P8, *Sox9*-lineage cells encompass the majority of the HF, including the infundibulum (33), which likely includes *Krox20*-positive and lineage cells. Notably, the reported lineage tracing in their study does not extend beyond P21, leaving open the possibility of subsequently detecting *Sox9*-lineage cells in the IFE during prolonged analyses. This observation would align with our results, wherein *Krox20*-lineage cells

are not detected in the IFE until approximately P30-P40. Given the marked heterogeneity of *Krox20*-expressing cells observed in our scRNA-seq data, we propose that not all *Krox20*-expressing cells possess the same degree of multipotency. It is conceivable that only a subset of *Krox20*-positive cells contributes to the IFE and differs from those contributing to the HF. For this reason, labeling most cells with varying multipotencies at the onset of lineage tracing may more accurately determine the fate of this heterogeneous cell population. Conversely, conducting lineage tracing at the clonal level may not accurately reflect the full capabilities or characteristics of the broader cell population, even when multiple replicates are performed. This discrepancy may contribute to the differences observed in our lineage tracing results with *Krox20-CreERT* in this study compared to the *Lrig1-CreERT* line reported by Page et al. (4), despite the extensive overlap between these two stem cell populations (Figures 1C and 4D). As part of our future research directions, we intend to differentiate between these distinct populations of *Krox20*-positive cells through additional lineage tracing experiments.

Our findings hold important implications for future studies to understand mechanisms that regulate epidermal homeostasis. In addition, our findings set the stage to investigate the contributions of *Krox20*-positive cells and their lineages in skin health and disease, with potential applications for skin repair following injury and burns.

Material and Methods

Mice

Sex as a biological variable: Our study examined male and female animals, and similar findings are reported for both sexes.

Krox20-Cre (35) (strain #025744), *K14-CreERT* (36) (strain #005107), *R26-tdTomato* (strain #007914) and *R26-YFP* (Strain #006148) mice were purchased from the Jackson Laboratory. *Krox20-flox-GFP-flox-DTA* mice (10) were a gift from Patrick Charnay (Mondor Institute for Biomedical Research, Creteil, France) and Piotr Topilko (Institut de Biologie de l'Ecole Normale Supérieure, Paris, France); *Krox20-flox-GFP-flox-DTA* functions as a knock-in allele, where GFP acts as a reporter for the *Krox20* promoter in the absence of Cre. When Cre is present, GFP is excised, and DTA is expressed to ablate the cells. In our study, we utilized *Krox20-GFP* to show the live expression of *Krox20*, while *Krox20-DTA* was employed when Cre was introduced to target and ablate *Krox20*-positive cells. *Krox20-CreERT* mice were generated by the Children's Research Institute (CRI) Transgenic Core at UT Southwestern.

Immunostaining

For immunofluorescence staining, frozen sections or paraffin sections after deparaffinization, rehydration, and antigen retrieval were used. The primary antibodies used in this study were: CD3 (B67, ab16669, Abcam); CD4 (ab183685, Abcam); CD8α (PA5-81344, Invitrogen); GFP/YFP (1020, Aves Labs); IBA1 (019-19741, Wako); CRE (NB100-56133, Novusbio), K14 (NBP234675B, biotin-labeled, Novus); K15 (ab52816, Abcam); Ki67 (15580, Abcam); KROX20 (PRB-236P, Covance; or 27814, Invitrogen; or 13491-1-AP, Protein Tech); Loricrin (905101, BioLegend); RFP/tdTomato (600-401-379S, Rockland). For immunofluorescence staining, the primary antibodies were visualized using secondary antibodies or streptavidin labeled with Cy3 or Alexa Fluor 488 (Jackson ImmunoResearch), with DAPI (Vector Labs) used for nuclei counterstaining.

Microscopy

Fluorescence microscopy images were captured using an Olympus fluorescence microscope (Model IX73) and the cell Sens Standard software (version 1.8). Image processing was conducted using Adobe Photoshop CS6 (version 13.0.1 x32), with adjustments limited to overall brightness/contrast and multi-color channel overlay. Statistical analysis was carried out using GraphPad Prism 8.

Quantification and statistical analysis

The statistical analysis was conducted using two-way ANOVA with GraphPad Prism 8. The data are presented as mean ± SEM. A *P* value of less than 0.05 was considered statistically significant. Significant differences were denoted by asterisks (*P < 0.05; **P < 0.01; ***P < 0.001; ****P < 0.0001).

Preparation of spatial transcriptomics libraries

Tissue optimization for mice at P38 was performed using Visium Spatial Tissue Optimization Slide & Reagent Kit (PN-1000193) following the manufacturer's protocol (document number CG000238_VisiumSpatialGeneExpression). Fresh-frozen skin tissues from three *Krox20-CreERT; R26-tdTomato* mice at P38 were cut into 10-um sections, and placed on slides from the Visium Spatial Gene Expression Slide & Reagent kit (10X Genomics, PN-1000187), fixed, H&E stained and imaged following the manufacturer's instructions (document number CG000160, 10X Genomics). Whole slide digital images of full tissue sections were taken at 20X magnification using a Zeiss Axioscan.Z1 slide scanner in the Whole Brain Microscopy Facility at UT Southwestern Medical Center (RRID:SCR_017949), and images were visualized with Zeiss Zen

Lite software (Blue version). Tissue permeabilization was performed for 12 minutes using Visium Spatial Tissue Optimization Slide & Reagent Kit (PN-1000193). Sequencing libraries were prepared following the manufacturer's instructions (document number CG000239_VisiumSpatialGeneExpression) followed by deep next generation sequencing in the Microbiome Core Facility at UT Southwestern Medical Center. Novaseq6000 sequencer was used to sequence the samples and loaded on one lane of XP S4 Flow cells PE-150.

Cell Lines

HEK293T cells were purchased from ATCC (Catalog #CRL-1573). Human hair follicular keratinocytes (HHFK) were purchased from ScienCell (2440, ScienCell).

***Krox20* Overexpression**

A lentiviral vector was generated by cloning the mouse *Krox20* cDNA (MR227610L4, OriGene) into a pLVX lentiviral backbone that also contains IRES-ZsGreen1 (631982, Clontech/ now Takara). Subsequently, HEK293T and HHFK cells were transfected with the lentiviral vector overexpressing mouse *Krox20.* Transfected cells were FACS sorted for fluorescent cells.

Western Blot

Cell lysates were subjected to western blot analysis, using the following antibodies: KROX20 (13491-1-AP, Protein Tech); BIM (2933, Cell Signaling); Cleaved Caspase-3 (9661, Cell Signaling); and GAPDH (SC-32233, Santa Cruz).

RT- qPCR

RT-qPCR was performed on the various cells using the following primers:

Notch1-Fwd: CACAACGAGGTCGGCTCCTA;

Notch1-Rvs: ACAGTTCTGGCCGGTGAAG;

B-catenin-Fwd: GACGGAGGAAGGTCTGAGGA;

B-catenin-Rvs: TGGCCATGTCCAACTCCATC;

Snail1-Fwd: TAATCCAGAGTTTACCTTCCAGCA;

Snail1-Rvs: AGCCTTTCCCACTGTCCTCA;

Snail2-Fwd: GCCAAACTACAGCGAACTGG;

Snail2-Rvs: AGGAGGTGTCAGATGGAGGA;

Twist1-Fwd: GGACAGTGATTCCCAGACGG;

Twist1-Rvs: CATAGTGATGCCTTTCCTTTCAG;

E-Cadherin-Fwd: CACCACGGGCTTGGATTTTG;

E-Cadherin-Rvs: CAGCCAGTTGGCAGTGTCTC;

GAPDH-Fwd: AGGGCTGCTTTTAACTCTGGT;

GAPDH-Rvs: CCCCACTTGATTTTGGAGGGA;

4-Hydroxytamoxifen and tamoxifen induction

To induce *Krox20*-lineage cell depletion in *Krox20-DTA; K14-CreERT* mice, adult mice received tamoxifen (2 mg) orally once daily for three consecutive days. For lineage tracing with *Krox20-CreERT; R26-tdTomato* mice, adult mice were orally administered tamoxifen (1 mg) once daily for three consecutive days. Perinatal induction involved a single injection of 4-hydroxytamoxifen (40 μg) at the tail junction of 1 to 3-day-old pups.

Genome-wide transcriptome analysis of *Krox20* at the single-cell level

Epithelial cells from epidermis of P5 *Krox20-GFP* mice were harvested following separation of the dermis from the epidermis by overnight incubation with dispase, as described in established protocols(37-39) and FACS sorted for *GFP*-positive (*Krox20*-expressing) cells using FACS Aria II SORP-5 lasers (PPMS for the Moody Foundation Flow Cytometry Facility at UTSW). Single cell suspensions were loaded with Single Cell 3' Gel Beads into a Next GEM Chip G and run on the Chromium™ Controller. Read one primer sequence was added during incubation and full-length, barcoded cDNA was then amplified by PCR after cleanup. Sample size was checked and then enzymatically fragmented and size-selected before proceeding to library construction. Post library preparation quality control was performed using the DNA 1000 tape on the Agilent TapeStation 4200. Samples were loaded at 1.8 pM and run on the Illumina NextSeq500 High Output Flowcell using V2.5 chemistry.

scRNA-seq data analysis

The analysis of single-cell transcriptomes was conducted using Cell Ranger 5.0.1 (10x Genomics, https://www.10xgenomics.com/). Raw sequencing data in BCL format were converted to FASTQ files and aligned to a custom mouse (mm10) reference transcriptome generated with cellranger mkref. Transcript counts for each cell were quantified using unique molecular identifiers and valid cell barcodes. The gene expression matrix from Cell Ranger was then input into the Seurat R package (v 4.0.5) for downstream analysis (53). Cells with fewer than 250 genes per cell and high mitochondrial gene content were filtered out. The LogNormalize method was used for global-scaling normalization. Highly variable genes were identified using the FindVariableFeatures module. The Shared Nearest Neighbor (SNN) graph was constructed with the FindNeighbors module by determining the k-nearest neighbors of each cell. Clusters were identified by optimizing

SNN modularity using the FindClusters module, resulting in 10 clusters with a resolution of 0.6. Differential expression analysis, cluster visualization, and plotting were performed using Seurat.

Study Approval

Mouse care and experiments were approved by the Institutional Animal Care and Use Committee at University of Texas Southwestern Medical Center and University of Virginia School of Medicine.

Acknowledgments

We thank Yong Wang for technical assistance, and all members of the Le laboratory for helpful suggestions and discussions. We thank Tripti Sharma of the Mouse Genome Engineering Facility at UT Southwestern's Children's Research Institute for assistance with generating the *Krox20-CreERT* mice. We also thank Drs. Patrick Charnay and Piotr Topilko at INSERM for generously providing mice. ET was supported by the National Cancer Institute of the National Institutes of Health under Award Number 3R01CA166593-07S1 and received a UTSW Hamon Center for Regenerative Science and Medicine Fellowship Award. EG was supported by the UTSW Dermatology Research Training Program T32 Grant T32AR065969. CPL was supported by the Career Development Award from the Dermatology Foundation. LQL held a Career Award for Medical Scientists from the Burroughs Wellcome Fund and the Kenneth E. Greer, M.D. Endowed Professorship at UVA School of Medicine. This work was supported by funding from the National Institutes of Health grant number R01CA166593 and R01EY033344 to LQL.

Contributions

L.Q.L. conceived and designed this research; E.G., E.T, T.S., Z.C., and Y.Z. performed experiments; L.Q.L., C.P.L., E.G., E.T. Z.Y., C.X. analyzed data; E.G. and R.M.M. wrote the paper; L.Q.L. oversaw the entire study. All authors read and approved the manuscript.

Data Availability

All data generated in this study are provided in the Supplementary Information/Source Data files. The single-cell RNA-seq data and spatial transcriptomics data discussed in this publication have been deposited in NCBI's Gene Expression Omnibus database, GSE281669 and GSE281086, respectively. Values for relevant figures are included with this manuscript as a supplemental Supporting Data Values file.

References

1. Blanpain C, and Fuchs E. Epidermal homeostasis: a balancing act of stem cells in the skin. *Nat Rev Mol Cell Biol.* 2009;10(3):207-17.
2. Clayton E, et al. A single type of progenitor cell maintains normal epidermis. *Nature.* 2007;446(7132):185-9.
3. Mascre G, et al. Distinct contribution of stem and progenitor cells to epidermal maintenance. *Nature.* 2012;489(7415):257-62.
4. Page ME, et al. The epidermis comprises autonomous compartments maintained by distinct stem cell populations. *Cell Stem Cell.* 2013;13(4):471-82.
5. Fuchs E, and Weber K. Intermediate filaments: structure, dynamics, function, and disease. *Annu Rev Biochem.* 1994;63:345-82.

6. Matsuki M, et al. Defective stratum corneum and early neonatal death in mice lacking the gene for transglutaminase 1 (keratinocyte transglutaminase). *Proc Natl Acad Sci U S A.* 1998;95(3):1044-9.

7. Ghotbi E, et al. Transcription factor KROX20 marks epithelial stem cell ancestors for hair follicle formation. *J Clin Invest.* 2024;134(23).

8. Liao CP, et al. Identification of hair shaft progenitors that create a niche for hair pigmentation. *Genes Dev.* 2017;31(8):744-56.

9. Gambardella L, et al. Pattern of expression of the transcription factor Krox-20 in mouse hair follicle. *Mech Dev.* 2000;96(2):215-8.

10. Vermeren M, et al. Integrity of developing spinal motor columns is regulated by neural crest derivatives at motor exit points. *Neuron.* 2003;37(3):403-15.

11. Li L, et al. Nestin expression in hair follicle sheath progenitor cells. *Proc Natl Acad Sci U S A.* 2003;100(17):9958-61.

12. Amoh Y, et al. Multipotent nestin-expressing hair follicle stem cells. *J Dermatol.* 2009;36(1):1-9.

13. Snippert HJ, et al. Lgr6 marks stem cells in the hair follicle that generate all cell lineages of the skin. *Science.* 2010;327(5971):1385-9.

14. Fullgrabe A, et al. Dynamics of Lgr6(+) Progenitor Cells in the Hair Follicle, Sebaceous Gland, and Interfollicular Epidermis. *Stem Cell Reports.* 2015;5(5):843-55.

15. Alvarez-Aznar A, et al. Tamoxifen-independent recombination of reporter genes limits lineage tracing and mosaic analysis using CreER(T2) lines. *Transgenic Res.* 2020;29(1):53-68.

16. Jensen KB, et al. Lrig1 expression defines a distinct multipotent stem cell population in mammalian epidermis. *Cell Stem Cell.* 2009;4(5):427-39.

17. Ito M, et al. Stem cells in the hair follicle bulge contribute to wound repair but not to homeostasis of the epidermis. *Nat Med.* 2005;11(12):1351-4.

18. Liu Z, et al. Systematic comparison of 2A peptides for cloning multi-genes in a polycistronic vector. *Sci Rep.* 2017;7(1):2193.

19. Ford NC, et al. Hair follicles modulate skin barrier function. *Cell Rep.* 2024;43(7):114347.

20. Dassule HR, et al. Sonic hedgehog regulates growth and morphogenesis of the tooth. *Development.* 2000;127(22):4775-85.

21. Lloyd C, et al. The basal keratin network of stratified squamous epithelia: defining K15 function in the absence of K14. *J Cell Biol.* 1995;129(5):1329-44.

22. Liu Y, et al. Keratin 15 promoter targets putative epithelial stem cells in the hair follicle bulge. *J Invest Dermatol.* 2003;121(5):963-8.

23. Zhang X, et al. Notch1 induces epithelial-mesenchymal transition and the cancer stem cell phenotype in breast cancer cells and STAT3 plays a key role. *Int J Oncol.* 2015;46(3):1141-8.

24. Xu J, et al. TGF-beta-induced epithelial to mesenchymal transition. *Cell Res.* 2009;19(2):156-72.

25. Mahmood MQ, et al. beta-catenin, Twist and Snail: Transcriptional regulation of EMT in smokers and COPD, and relation to airflow obstruction. *Sci Rep.* 2017;7(1):10832.

26. Cano A, et al. The transcription factor snail controls epithelial-mesenchymal transitions by repressing E-cadherin expression. *Nat Cell Biol.* 2000;2(2):76-83.

27. Takeichi M. Morphogenetic roles of classic cadherins. *Curr Opin Cell Biol.* 1995;7(5):619-27.

28. Huber O, et al. Cadherins and catenins in development. *Curr Opin Cell Biol.* 1996;8(5):685-91.

29. Taylor G, et al. Involvement of follicular stem cells in forming not only the follicle but also the epidermis. *Cell.* 2000;102(4):451-61.

30. Levy V, et al. Epidermal stem cells arise from the hair follicle after wounding. *FASEB J.* 2007;21(7):1358-66.

31. Brownell I, et al. Nerve-derived sonic hedgehog defines a niche for hair follicle stem cells capable of becoming epidermal stem cells. *Cell Stem Cell.* 2011;8(5):552-65.

32. Blanpain C, and Fuchs E. Stem cell plasticity. Plasticity of epithelial stem cells in tissue regeneration. *Science.* 2014;344(6189):1242281.

33. Nowak JA, et al. Hair follicle stem cells are specified and function in early skin morphogenesis. *Cell Stem Cell.* 2008;3(1):33-43.

34. Levy V, et al. Distinct stem cell populations regenerate the follicle and interfollicular epidermis. *Dev Cell.* 2005;9(6):855-61.

35. Voiculescu O, et al. Expression pattern of a Krox-20/Cre knock-in allele in the developing hindbrain, bones, and peripheral nervous system. *Genesis.* 2000;26(2):123-6.

36. Vasioukhin V, et al. The magical touch: genome targeting in epidermal stem cells induced by tamoxifen application to mouse skin. *Proc Natl Acad Sci U S A.* 1999;96(15):8551-6.

37. Rendl M, et al. Molecular dissection of mesenchymal-epithelial interactions in the hair follicle. *PLoS Biol.* 2005;3(11):e331.

38. Zhang LJ. Isolation, Culture, and Characterization of Primary Mouse Epidermal Keratinocytes. *Methods Mol Biol.* 2019;1940:205-15.

39. Li F, et al. Isolation and Culture of Primary Mouse Keratinocytes from Neonatal and Adult Mouse Skin. *J Vis Exp.* 2017(125).

Figure 1

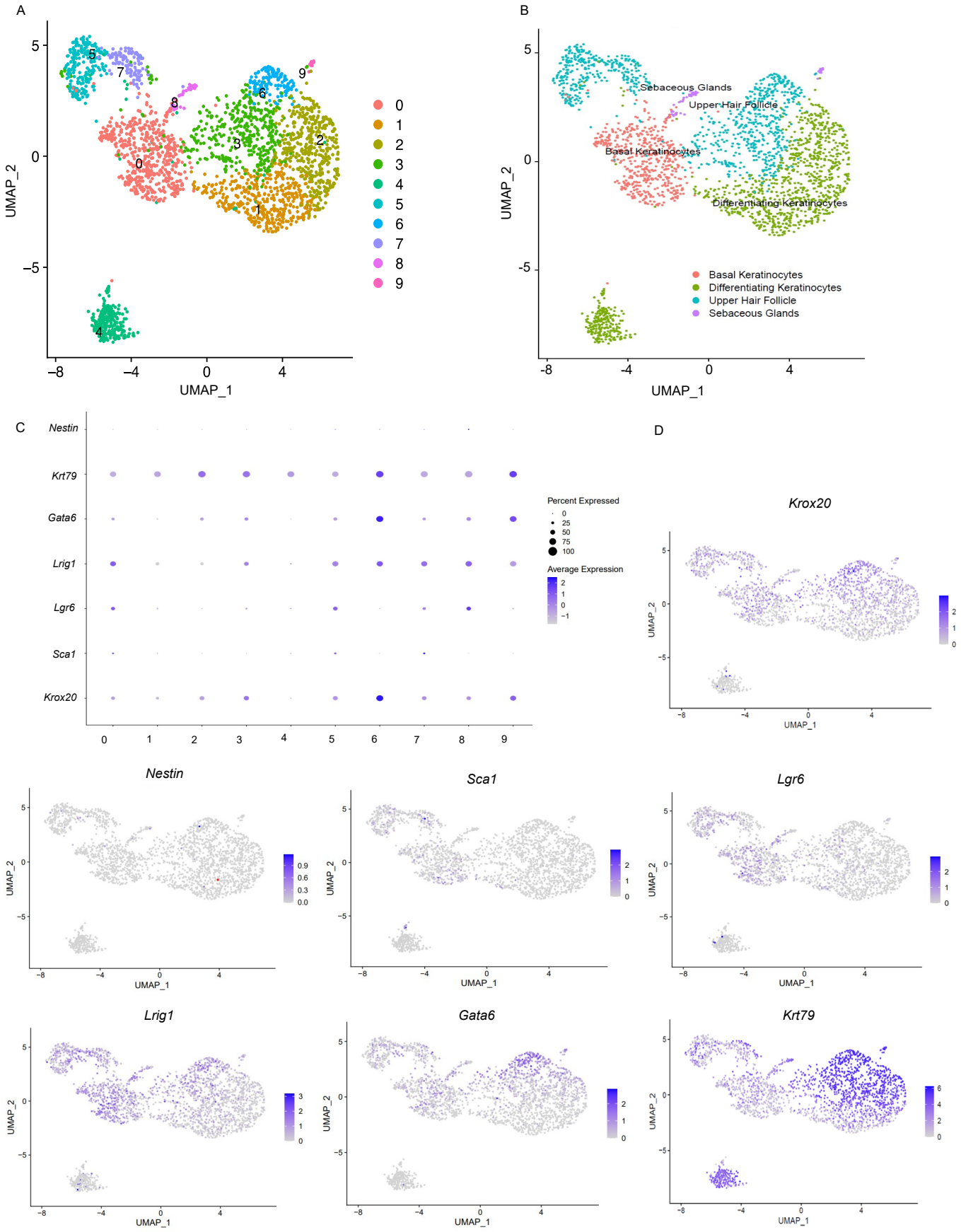
A
B
C
D
UMAP_1
UMAP_2
Sebaceous Glands
Upper Hair Follicle
Basal Keratinocytes
Differentiating Keratinocytes
Basal Keratinocytes
Differentiating Keratinocytes
Upper Hair Follicle
Sebaceous Glands
Nestin
Krt79
Gata6
Lrig1
Lgr6
Sca1
Krox20
Percent Expressed
Average Expression
Krox20
Nestin
Sca1
Lgr6
Lrig1
Gata6
Krt79

Figure 1. scRNA-seq analysis on the epidermal cells of *Krox20-GFP* P5 pups reveals cellular heterogeneity of *Krox20*-expressing cells. (**A**) UMAP representation of the transcriptomes of *Krox20*-expressing cells with annotated clusters (n = 5). 10 clusters of differentially expressed cells were identified. (**B**) Cell type annotations of the clusters identified. (**C**) Dot plot showing expression of *Nestin, Krt79*, *Gata6*, *Lrig1*, *Lgr6*, *Sca1 (Ly6a)*, and *Krox20* in annotated clusters. (**D**) Expression of *Krox20*, *Nestin, Sca1*, *Lgr6, Lrig1*, *Gata6,* and *Krt79* visualized on UMAP. Color intensity from gray to blue shows the expression level for each gene.

Figure 2

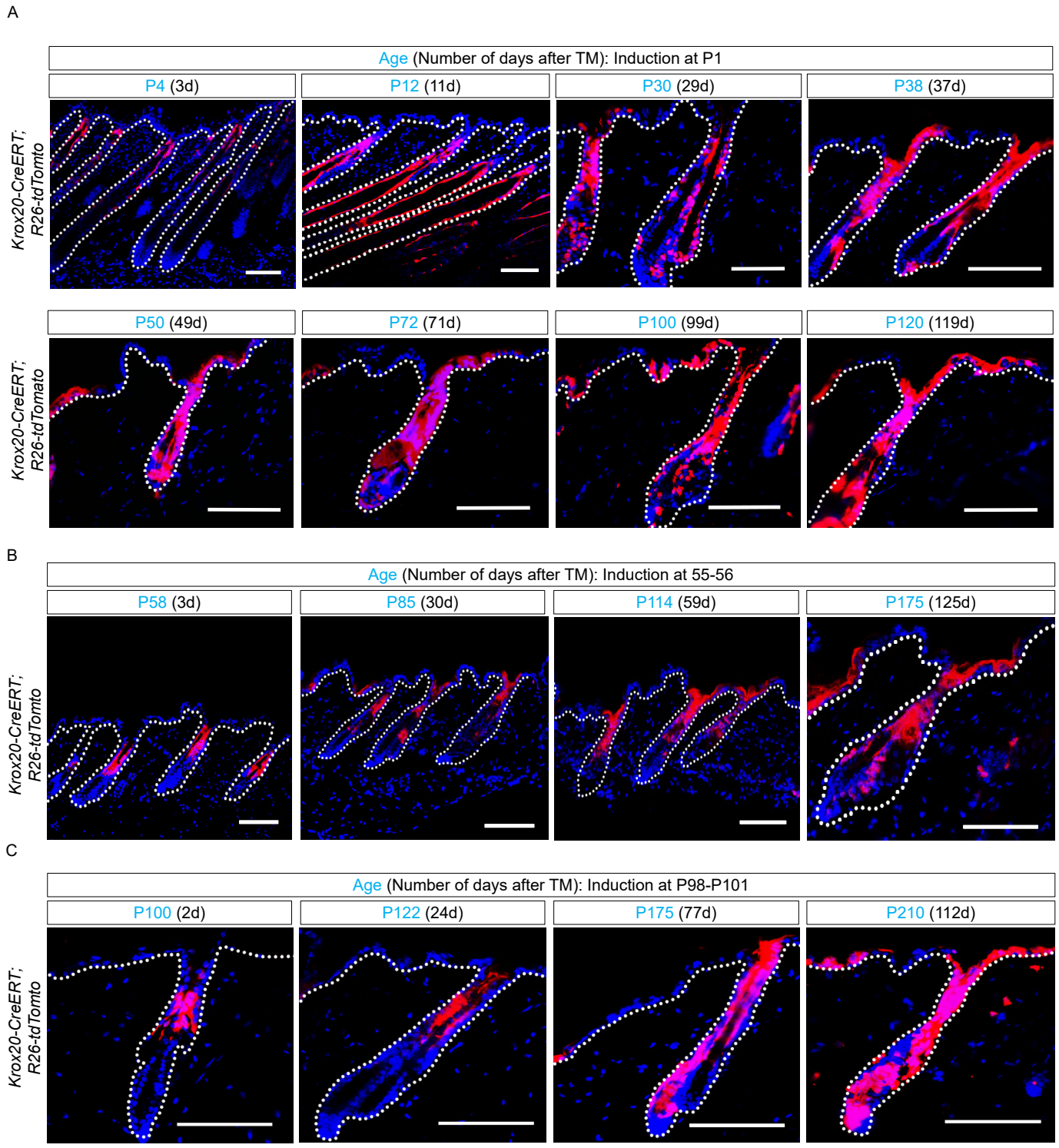
A
Age (Number of days after TM): Induction at P1
P4 (3d)
P12 (11d)
P30 (29d)
P38 (37d)
Krox20-CreERT; R26-tdTomto
P50 (49d)
P72 (71d)
P100 (99d)
P120 (119d)
Krox20-CreERT; R26-tdTomato
B
Age (Number of days after TM): Induction at 55-56
P58 (3d)
P85 (30d)
P114 (59d)
P175 (125d)
Krox20-CreERT; R26-tdTomto
C
Age (Number of days after TM): Induction at P98-P101
P100 (2d)
P122 (24d)
P175 (77d)
P210 (112d)
Krox20-CreERT; R26-tdTomto

Figure 2. Lineage tracing in *Krox20-CreERT; R26-tdTomato* mice reveals contribution of *Krox20*-lineage cells to the IFE. (**A - C**) Lineage tracing initiated at P1 (**A**), P55 (**B**), and P98 (**C**) shows *Krox20*-lineage cells contribute to the HF and IFE over time. $n \geq 3$. Scale bar, 100 μm.

Figure 3

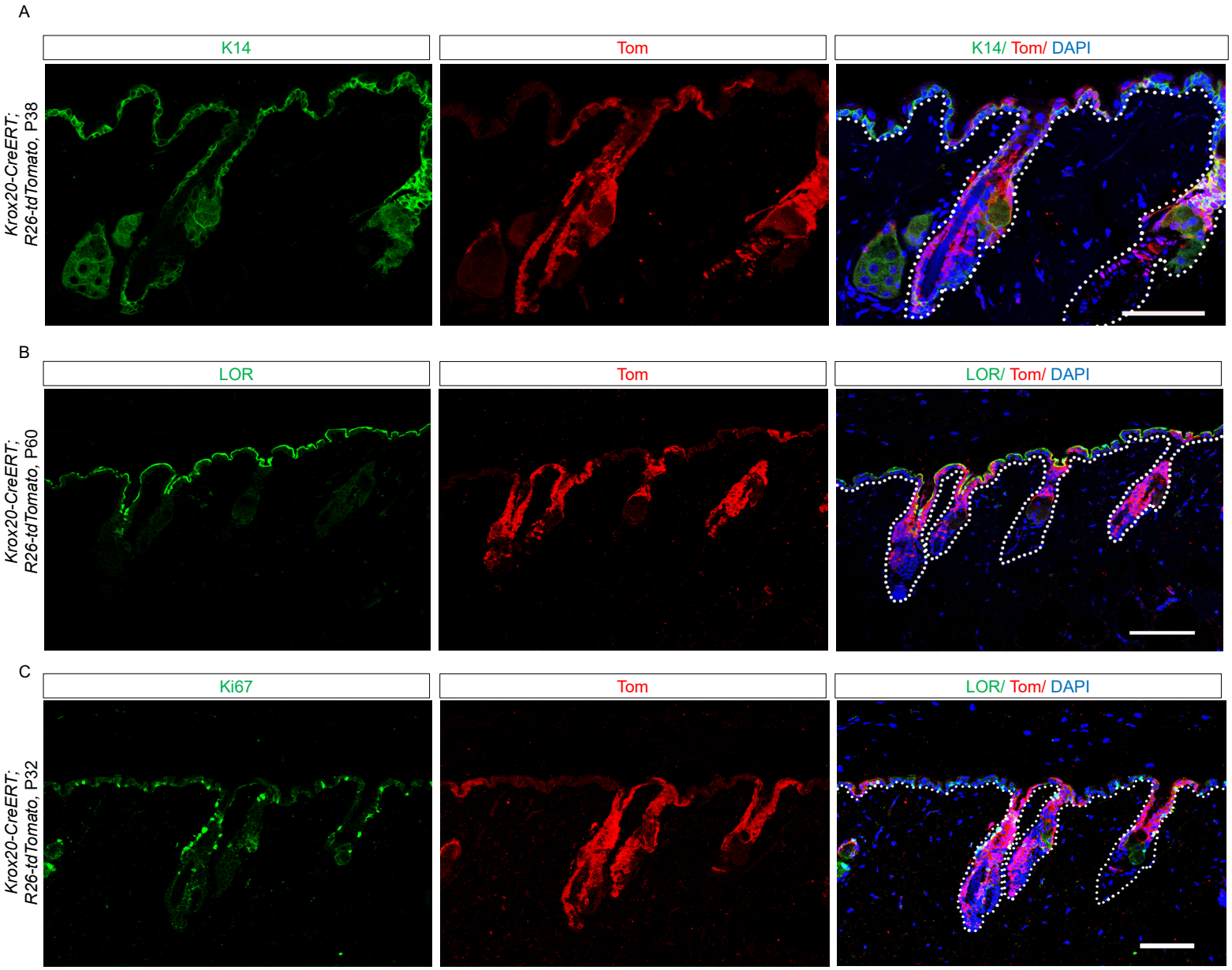
A
K14
Tom
K14/ Tom/ DAPI
Krox20-CreERT;
R26-tdTomato, P38
B
LOR
Tom
LOR/ Tom/ DAPI
Krox20-CreERT;
R26-tdTomato, P60
C
Ki67
Tom
LOR/ Tom/ DAPI
Krox20-CreERT;
R26-tdTomato, P32

Figure 3. *Krox20*-lineage cells overlap with IFE and bulge markers. (**A-C**) Co-localization analysis demonstrates the detection of Tom-labeled *Krox20*-lineage cells (TOM = *tdTomato*) in relation to the K14 marker of basal layer of IFE (**A**), the Loricrin (Lor) marker of suprabasal granular layer (**B**), and the Ki67 marker of proliferating cells (**C**) in telogen HFs at P38, P60, and P32, respectively, induced at P1. $n \geq 4$. Scale bar, 100 μm.

Figure 4

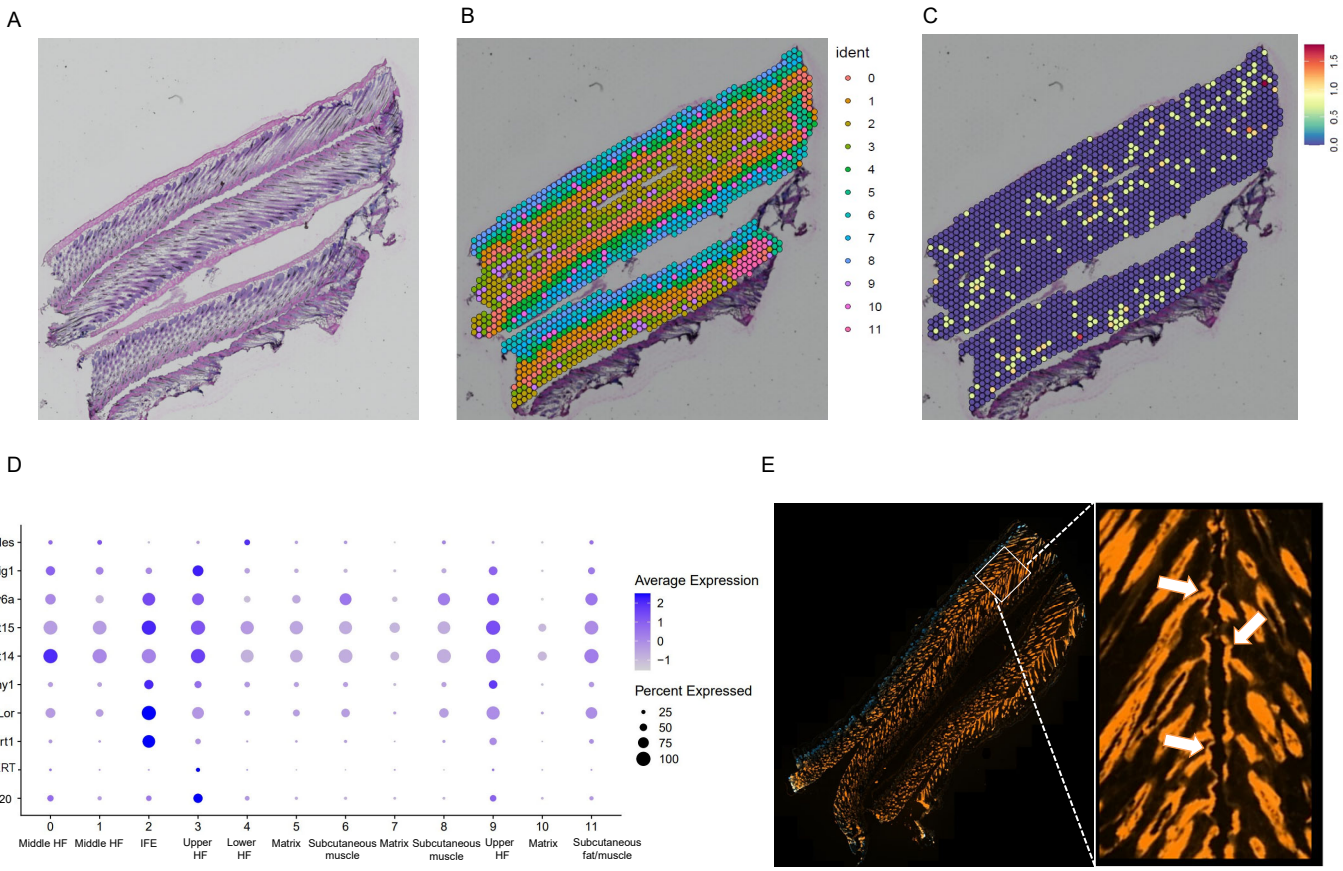
A
B
C
ident
0
1
2
3
4
5
6
7
8
9
10
11
0.0
0.5
1.0
1.5
D
Nes
Lrig1
Ly6a
Krt15
Krt14
Thy1
Lor
Krt1
CreERT
Krox20
0
1
2
3
4
5
6
7
8
9
10
11
Middle HF
Middle HF
IFE
Upper HF
Lower HF
Matrix
Subcutaneous muscle
Matrix
Subcutaneous muscle
Upper HF
Matrix
Subcutaneous fat/muscle
Average Expression
2
1
0
−1
Percent Expressed
25
50
75
100
E

Figure 4. Spatial transcriptomic analysis of the dorsal skin of *Krox20-CreERT; R26-tdTomato* mice at P38. (**A**, **B**) Identification of 12 clusters of cells with differentially expressed genes, with cluster 1 representing the IFE. H&E-stained cross-sections of the skin, each section representing one mouse (n = 3, **A**). Note that the fourth section was excluded from analysis due to distorted structure. Spatial dim plots for all clusters (**B**). (**C**) Spatial feature plot for expression of *CreERT* is presented. Color intensity from blue to red shows the expression level for each gene. (**D**) Dot plots illustrating the expression levels of *Krox20*, *CreERT*, the marker of the upper and middle HF *Lrig1*, the marker of bulge stem cells *Nestin* (Nes), and IFE markers (*K14*, *K15*, *K1*, *Thy1*, *Sca1*, and *loricrin*) in the different gene clusters along with cluster annotations. (**E**) Live expression of *tdTomato* from the same four skin samples presented in **A**-**C**. White arrows point to the labeled HF mouth or IFE.

Figure 5

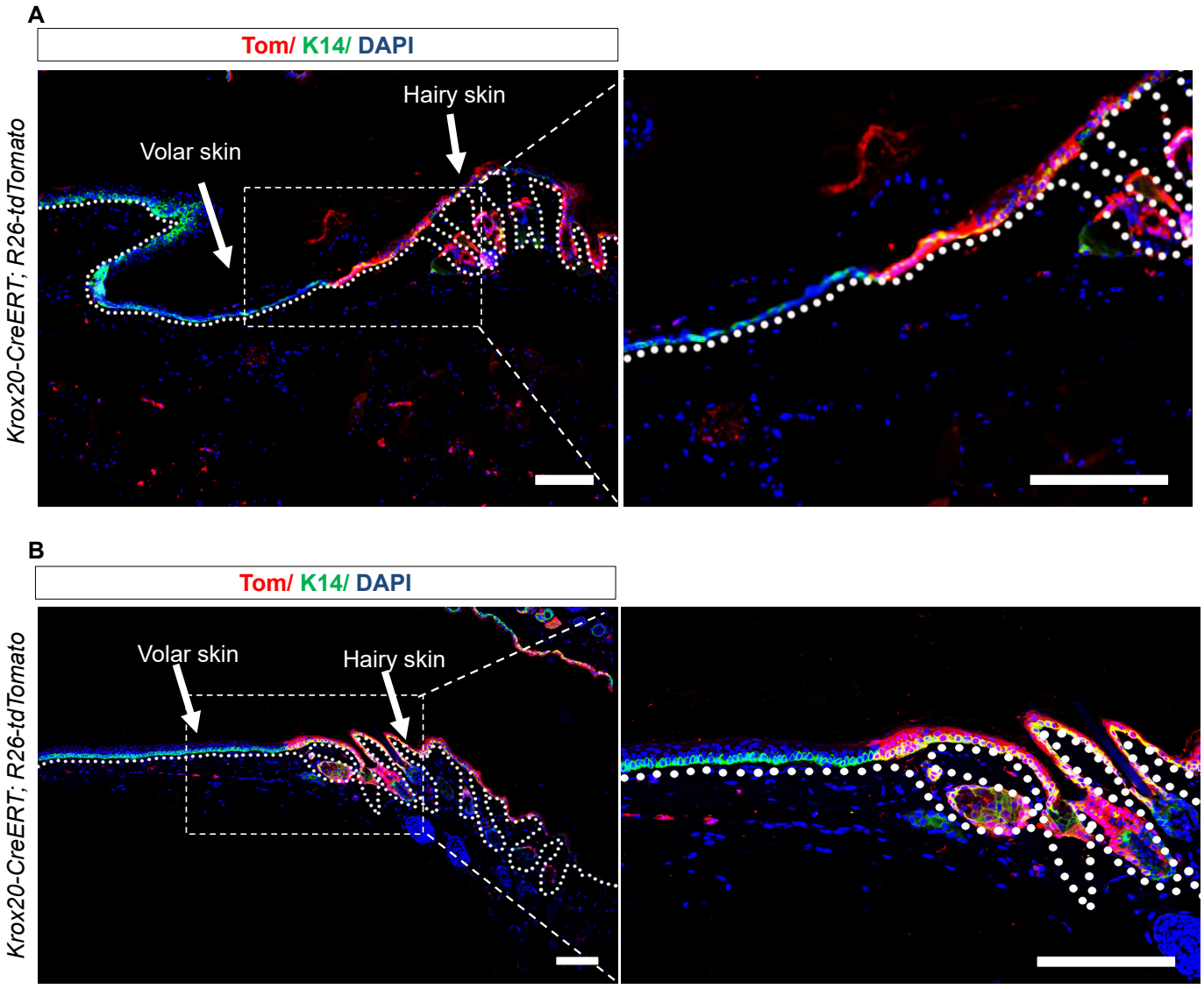
A
Tom/ K14/ DAPI
Hairy skin
Volar skin
Krox20-CreERT; R26-tdTomato
B
Tom/ K14/ DAPI
Volar skin
Hairy skin
Krox20-CreERT; R26-tdTomato

Figure 5. *Krox20* is not expressed in the volar epithelium. (**A, B**) Lineage tracing in 11-month-old *Krox20-CreERT; R26-tdTomato* mice, induced at P1 (**A**), and P158 mice, induced at P55 (**B**), shows the absence of *Krox20*-lineage cells in the volar epithelium of palmoplantar skin. n = 2. Scale bar,100 μm.

Figure 6

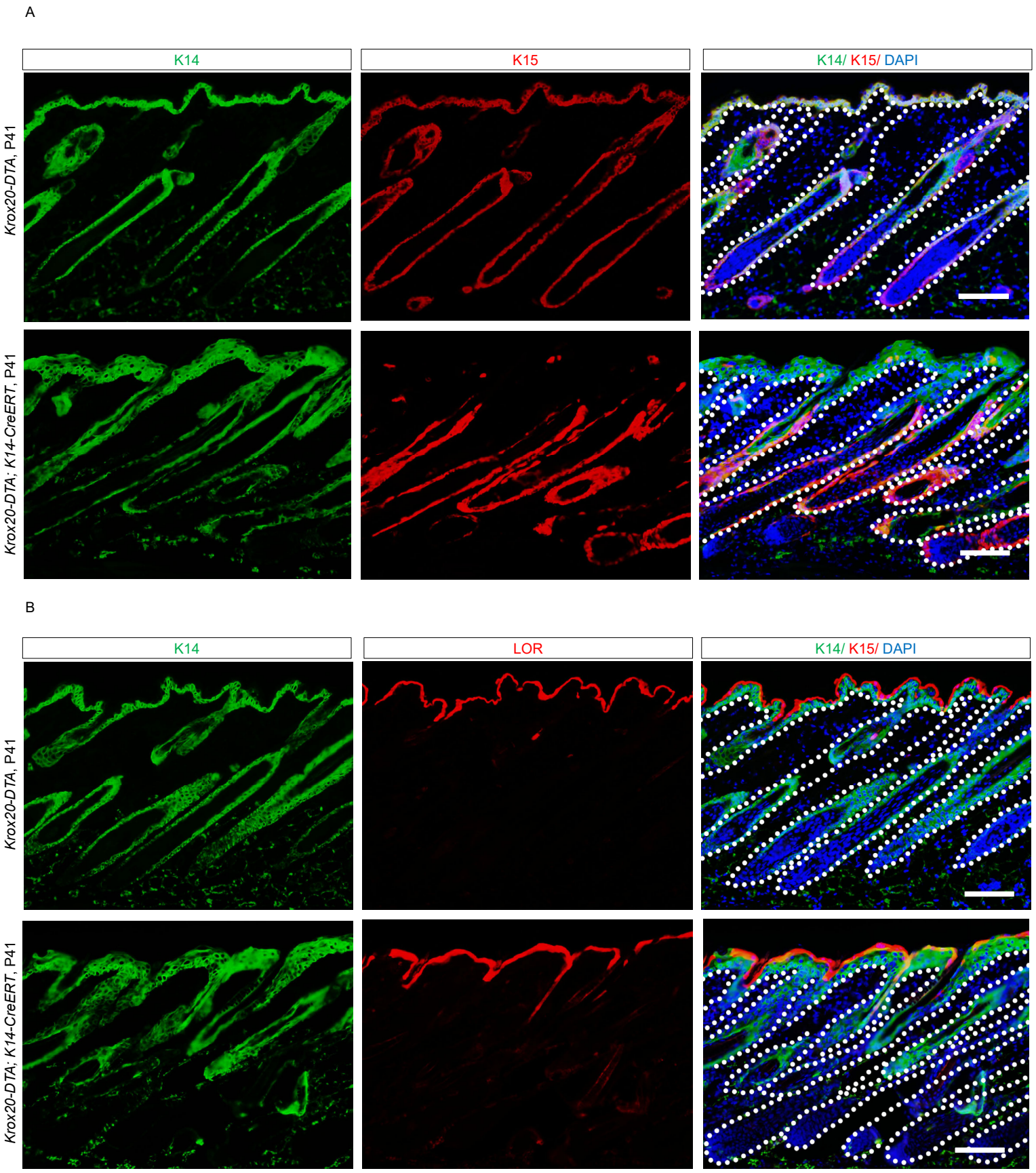
A
K14
K15
K14/ K15/ DAPI
Krox20-DTA, P41
Krox20-DTA; K14-CreERT, P41
B
K14
LOR
K14/ K15/ DAPI
Krox20-DTA, P41
Krox20-DTA; K14-CreERT, P41

Figure 6. *Krox20*-positive cells are indispensable for skin homeostasis. (**A**, **B**) Analysis of the skin of *Krox20-DTA; K14-CreERT* mice at P41 induced at P32 shows the disruption of skin homeostasis and stratification as indicated by the absence of K15 expression in the IFE (**A**), and overlap of the suprabasal marker Lor with the K14 basal marker in the IFE (**B**). n = 3. Scale bar, 100 μm.

Figure 7

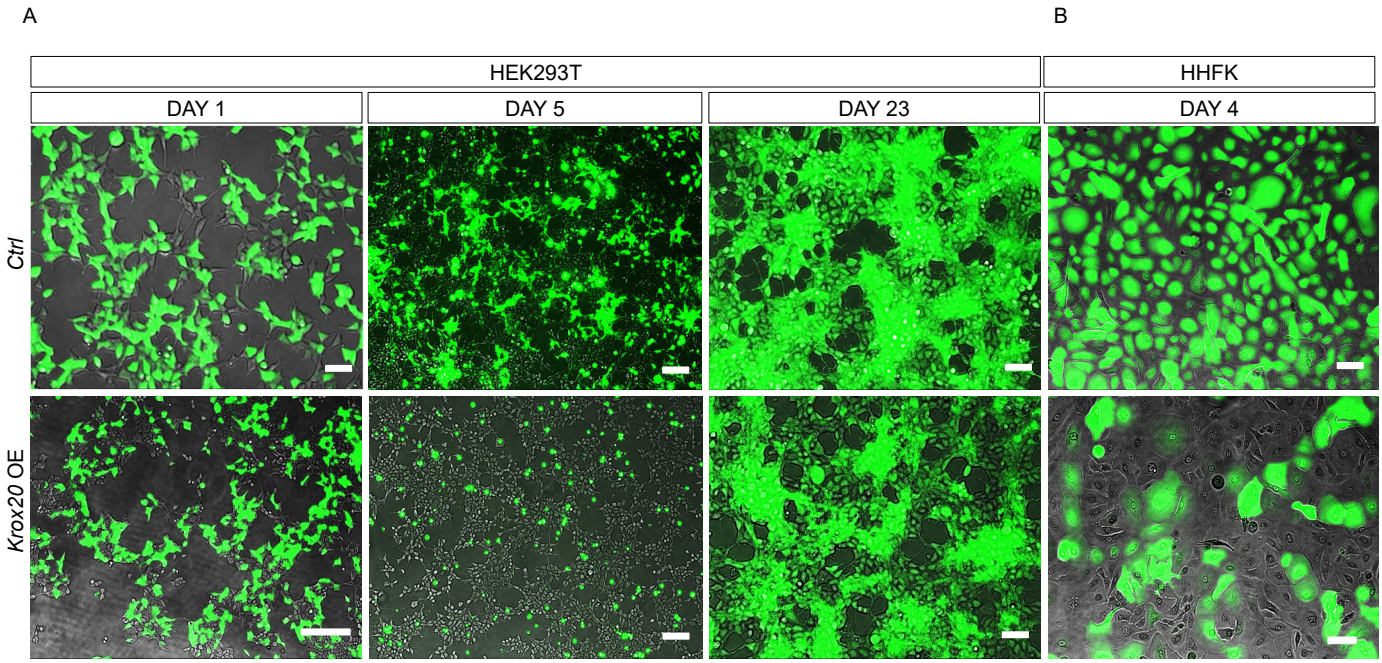
A
B
HEK293T
HHFK
DAY 1
DAY 5
DAY 23
DAY 4
Ctrl
Krox20 OE

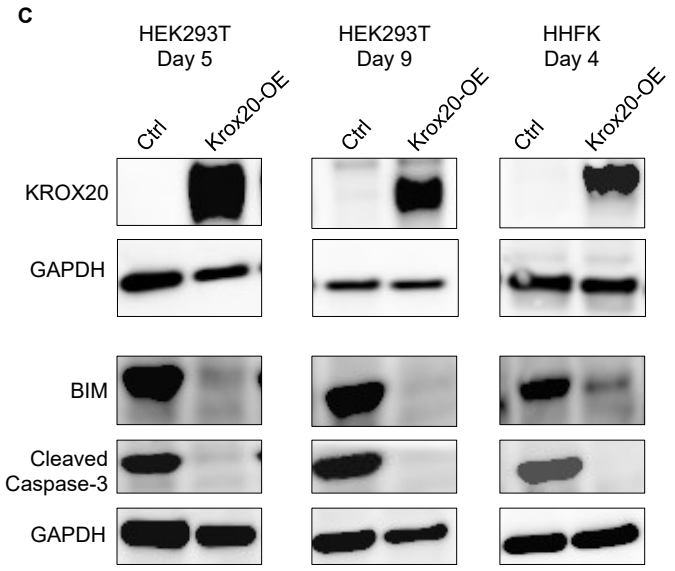
C
HEK293T
Day 5
HEK293T
Day 9
HHFK
Day 4
Ctrl
Krox20-OE
KROX20
GAPDH
BIM
Cleaved
Caspase-3
GAPDH

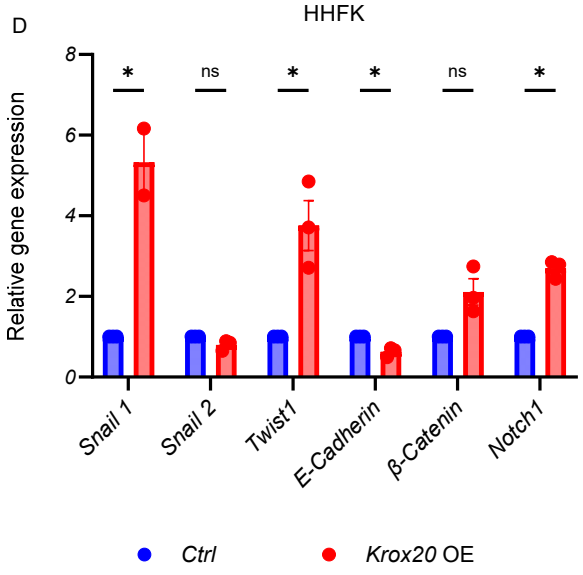
D
HHFK
Relative gene expression
8
6
4
2
0
*
ns
*
*
ns
*
Snail 1
Snail 2
Twist1
E-Cadherin
β-Catenin
Notch1
Ctrl
Krox20 OE

Figure 7. *Krox20* overexpression in vitro alters cell identity. Overexpression of *Krox20* (*Krox20*-OE) induces morphological changes in HEK293T cells (**A**), and a less pronounced change in HHFK cells (**B**). (**C**) Western blot analysis demonstrates downregulation of apoptotic markers in *Krox20*-OE cells. The same biological samples were run on a separate gel and probed for KROX20 and GAPDH. (**D**) qRT-PCR demonstrates that overexpression of *Krox20* results in upregulation of EMT regulators (*Snail1*, *Twist1*, *β-catenin*, and *Notch1*) and downregulation of the epithelial marker *E-Cadherin*. Results are normalized to *GAPDH*. n = 3 replicates per condition. Statistics represent mean ± SEM. Two-tailed Student's t-test, *P<0.05. ns: not significant. Scale bar, 100 μm.